World Conference on Timber Engineering Oslo 2023

# STUDY ON FRAME DESIGN OF CONVENTIONAL WOODEN HOUSE

**Tomoya Sahata[1], Naohito Kawai[2], Hideyo Tsukazaki[3]**

**ABSTRACT:** This study assesses conventional Japanese architectural methods. Japanese houses constitute a framework with columns and beams. In addition to these structures, braces are installed to provide resistance to earthquakes and wind loads. A brace wall consists of foundations, columns, beams, and braces. Members are produced from standing trees. Therefore, the member length is constrained. For this reason, the lengths of timbers distributed in the market are 3–6 m. For horizontal members such as beams, the ends of the members must be connected to provide the necessary length for the building. For this study, we confirmed the effects on the strength and failure properties when joints were provided on beams that make up the brace wall. Results indicate that the joint of the beam placed on the 910 mm brace wall did not affect the maximum load, but had a slightly reduced initial stiffness.

**KEYWORDS:** Beam joint, Brace wall, Factual investigation, In-plane shear test, Structural analysis

## 1 INTRODUCTION

A conventional Japanese wooden house is made up of wooden materials such as columns and beams (Fig. 1). For an average-sized house, a joint is necessary to extend the beam length. As a rule, this joint should not be placed inside the wall to which the brace is to be attached, as presented in Fig. 2 [1]. However, when performing seismic reinforcement work, it might be necessary to install a beam joint on the brace wall [2]. Our drawing survey [3] results revealed that many beam joints in braced walls exist, even in new houses. Reports of past studies have described many findings from examinations of braced walls and beam joints. For braced walls, the effects have been confirmed of different species of braces and different types of joint hardware at the end of the braces on strength properties [4, 5]. Regarding joints, the effects of different species of wood, cross-sectional dimensions, and shapes of the joints on joint performance have been confirmed [6, 7]. However, the effects on brace walls have not been clarified when the beam joint is installed in the brace wall. Therefore, this study was conducted to elucidate the effects of beam joints of braced walls on strength and fracture properties. As described herein, a questionnaire survey related to the arrangement of the joints was administered to frame designers. After the configurations of loading tests and structural analyses were found, the beam joint effects on the strength properties of braced walls were assessed.

[1] Tomoya Sahata, Polytechnic University, Japan (Kogakuin University Doctoral Program) t-sahata@uitec.ac.jp
[2] Naohito Kawai, Kogakuin University, Japan kawai-nk@cc.kogakuin.ac.jp
[3] Hideyo Tsukazaki, Polytechnic University, Japan tukazaki@uitec.ac.jp

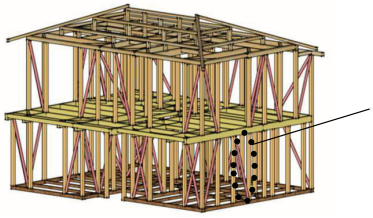

***Figure 1:*** *Shaft assembly model*

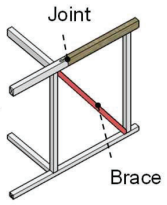


***Figure 2:*** *Joint of beam member in brace wall*

## 2 FACTUAL INVESTIGATON

### 2.1 OUTLINE OF THE ACTUAL SURVEY

A questionnaire survey was conducted of frame designers at wood processing (hereinafter, pre-cutting) factories with the aim of identifying trends in the arrangements of joints in beam members. The first survey targeted 108 pre-cutting factories with annual processing area of approximately 100,000 $m^2$ or more. The second survey was administered to 201 companies (including 64 pre-cutting factories targeted by the first survey) that mainly use software from three major pre-cut CAD manufacturers. The number of newly selected pre-cutting factories was 137. The total number of companies in the first and second surveys was 245. Table 1 presents results of the questionnaire collection. The combined collection rate for the first and second questionnaires was 24.1%. Interviews were conducted with 23 of the 68 respondents to assess their responses.

***Table 1:*** *Questionnaire collection results*

| Number | 1st time | 2nd time | Duplication | Total | Response rate Number of companies responding / Number of companies sent |
|---|---|---|---|---|---|
| Shipping companies | 108 | 201 | 64 | 245 | 59 companies/245 companies (%) 24.1 % |
| Answer companies | 24 | 35 | – | 59 | |
| Respondents | 24 | 44 | – | 68 | – |

### 2.2 LENGTH OF WOOD TO BE USED

Findings from the survey of the lengths of timber used for horizontal members are depicted in Fig. 3. Because the


https://doi.org/10.52202/069179-0449

same trend was observed for the horizontal structure of the first floor, second floor, and shed structures, they are presented together. As the figure shows, 4 m timber is the most commonly used material, followed by 3 m and 5 m. According to the interview survey, 3 m and 5 m timbers are used in the right places in relation to the positions of the columns and openings, perhaps because of the very low use of lumber longer than 6 m, the high price, and the reduced ease of installation on site.

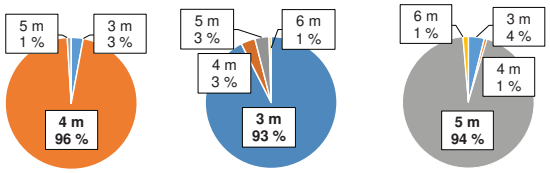


***Figure 3:*** *Priority of specified length of horizontal member to be used*

## 2.3 TYPES OF JOINTS FOR HORIZONTAL MEMBERS

Results of a survey of the types of connections used for horizontal members are portrayed in Fig. 4 for the first floor, second floor, and shed sections together. Fig. 4 shows that more than 70% use the type B joining method. The type A jointing method is also often used for horizontal structures of the first floor. Type A joints are often used in the horizontal structure of the first floor because the foundation and base are connected by anchor bolts, which require no high bending performance. Furthermore, interviews conducted after the questionnaires were collected also indicate construction-related reasons, such as easier on-site assembly.

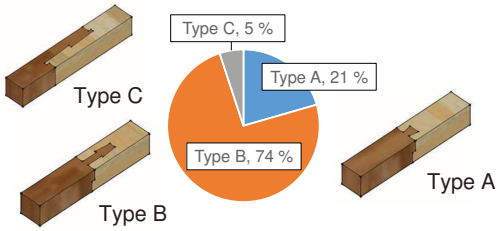


***Figure 4:*** *Types of beam joints in horizontal members*

## 2.4 JOINT OF HORIZONTAL MEMBERS PLACED IN THE BRACE WALL

A questionnaire survey was administered to ascertain the actual situation of the frame design work. The relative positions of the brace and the beam joints in the brace wall are presented in Fig. 5. Joints of the beam in the brace wall are of three types: push up of the single brace (Fig. 5(i)); the opposite side of the push up portion of the single brace (Fig. 5(ii)); and the push up portion of the double brace (Fig. 5(iii)). Results of these investigations of the beam joints in the brace walls are shown in Fig. 6. The percentages of designers who responded "give special consideration" or "give consideration" were 74% in the case of Fig. 6(i) and 80% in the case of Fig. 6(iii). Those findings indicate that more than 70% of the designers responded that they would "consider" or "give consideration" to the push up portion of the brace in the brace wall. However, the interview survey results suggest that beam joints had to be placed at the push-up of the braces sometimes to prioritize the yield of fixed-length materials (mainly 3 m and 4 m).

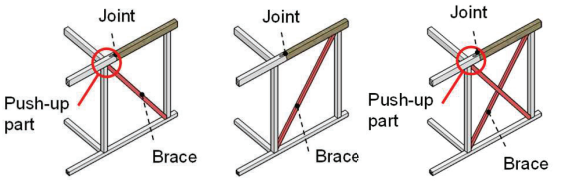


***Figure 5:*** *Positions of beams in joints of a brace wall*

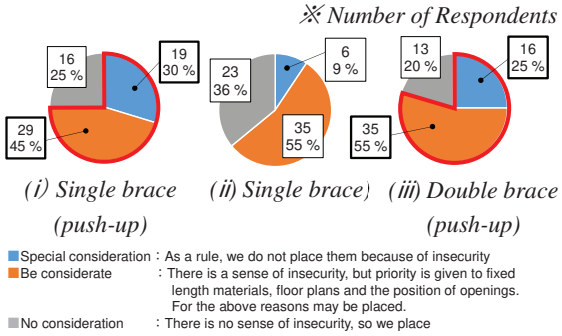


***Figure 6:*** *Awareness of beam joints on the inside of brace walls*

# 3 IN-PLANE SHEAR TEST

## 3.1 SPECIMEN AND TEST BODY

Table 2 presents the specifications of members that constitute the test body. Fig. 7 shows the test body configuration: cross-sectional dimensions of the foundation and column are 105 × 105 mm; the beam is 105 × 180 mm; the studs are 30 × 105 mm; and the brace is 45 × 90 mm. The test body dimensions indicate a 910 mm wall length and a 2730 mm wall height. It is noteworthy that the 910 mm test body length is a traditional Japanese unit. The test body parameters reflect how to set the brace and presence and absent joint. The test body name is the following.

[Test body name] A – B
A: How to set a brace
B: Presence or absence of beam joint

***Table 2:*** *List of physical properties of test materials*

| Material name | Tree species | Air-dry density (kg/m³) | Moisture content (%) | Average annual ring width (mm) | Young's modulus (kN/mm²) |
|---|---|---|---|---|---|
| Foundation | Cedar | 482 | 14 | 4.3 | 11.5 |
| Column | RW laminated wood | 496 | 14 | – | 11.5 |
| Beam | RW laminated wood | 471 | 15 | – | 10.5 |
| Brace | Cedar LVL | 369 | 11 | – | 8.3 |
| Stud | WW laminated wood | 432 | 11 | – | 11.8 |

Table 3 presents a legend for test body symbols. It lists the test bodies. The number of test bodies was three for each. The total of test bodies was 12.

https://doi.org/10.52202/069179-0449

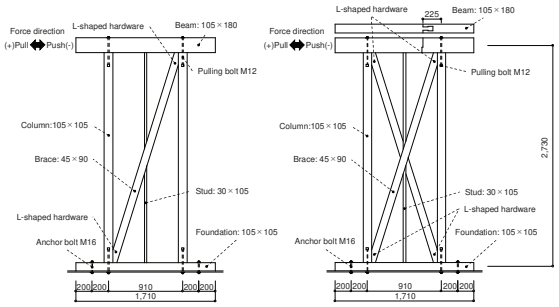


*Single brace / joint none* *Double brace / joint placed*

***Figure 7:*** *Configuration of In-plane shear test (unit: mm)*

***Table 3:*** *List of test bodies*

| Test body symbol | How to set a brace | Presence or absence of beam joint | Number of test bodies |
|---|---|---|---|
| SN | **S**ingle | **N**one | 3 |
| SJ | **S**ingle | **J**oint | 3 |
| DN | **D**ouble | **N**one | 3 |
| DJ | **D**ouble | **J**oint | 3 |

## 3.2 TEST METHOD

The test method was based on an allowable stress design for wood-frame housing [8]. The historical force was repeated three times with positive and negative alternating forces so that the apparent deformation angle became 1/450, 1/300, 1/200, 1/150, 1/100, 1/75, and 1/50 rad, as presented in Fig. 8. Then it was pulled until the apparent deformation angle became 1/15 rad. As presented in Fig. 9, the relative rotation angle between the upper member and lower member of the beam joint is calculated using the displacement of two electrical displacement meters attached to the beam joint.

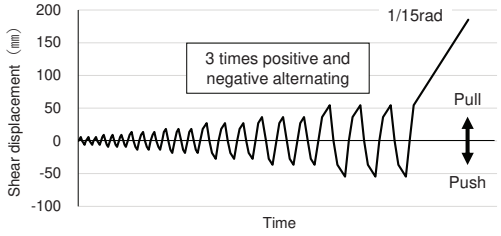


***Figure 8:*** *Loading schedule for in-plane shear test*

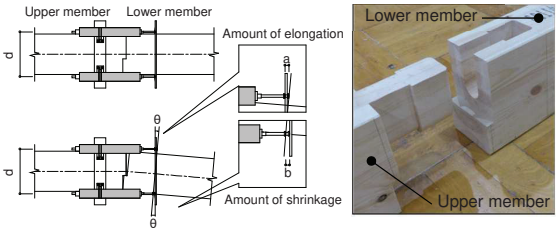


$\theta = ( a - b ) / d$

$\theta$: Relative displacement angle of two members (rad)

$a,b$: Displacement by displacement meter (mm)

$d$: Distance between gauge points (mm)

***Figure 9:*** *Method of rotation angle calculation for beam joint angles of beams joint*

## 3.3 TEST RESULTS AND DISCUSSION

Fig. 10 shows the relation between the load and the shear deformation angle. Table 4 presents the maximum load and initial stiffness as calculated from the test results presented in Fig. 10. The maximum load and initial stiffness of the test body of the single brace (SN) are greater than those of the SJ. For the test body of the double brace, the maximum load and initial stiffness of DN are comparable to those of DJ. Table 5 shows the rotation angle of the joints at maximum load. From Table 5, it is apparent that the angle of rotation of the joint at maximum load is greater for SJ than for DJ. This greater angle can be attributed to the difference in the magnitude of the moment generated at the beam joint by the brace. In the case of the double brace, because the compression brace is joined to the tension brace at the midpoint of the lengthwise direction of the material, one can infer that the force pushing up the beam is less than that of the single brace because of the relaxation of the compressive force. Fig. 11 shows the test body at 1/15 rad. From the left side of Fig. 11, it is apparent that no marked damage has occurred to the beam joints. This finding suggests that the effect of the beam joints on the maximum load of the braced wall is small. Regardless of the presence or absence of beam joints, the failure of all test bodies terminated in buckling of the compression brace, as shown on the right side of Fig. 11.

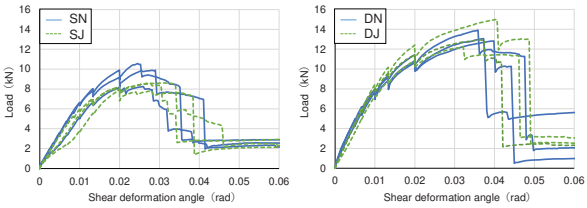


*Single brace wall* *Double brace wall*

***Figure 10*** *Relation between load and shear deformation angle*

***Table 4:*** *Structural property values when pulled*

| Test body name | Maximum load (kN) | | | | | Initial rigidity (kN/rad) | | | | |
|---|---|---|---|---|---|---|---|---|---|---|
| | No.1 | No.2 | No.3 | Average | Ratio | No.1 | No.2 | No.3 | Average | Ratio |
| SN | 10.6 | 8.3 | 9.9 | **9.6** | – | 663 | 510 | 673 | **615** | – |
| SJ | 8.0 | 8.6 | 8.6 | **8.4** | **0.88** | 634 | 477 | 424 | **512** | **0.83** |
| DN | 13.1 | 12.8 | 13.9 | **13.3** | – | 835 | 799 | 738 | **791** | – |
| DJ | 15.0 | 12.9 | 12.2 | **13.4** | **1.01** | 795 | 768 | 695 | **753** | **0.95** |

***Table 5:*** *Joint rotation angle at maximum load (rad)*

| No. | SJ | DJ |
|---|---|---|
| No.1 | 0.002 | 0.000 |
| No.2 | 0.008 | -0.001 |
| No.3 | 0.023 | 0.004 |
| Average | 0.011 | 0.001 |

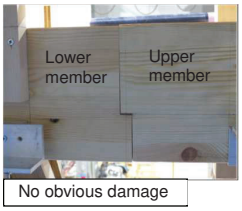



*State of the joint* *Viewed from the side*

***Figure 11:*** *State of the test body at 1/15 rad(SN)*


https://doi.org/10.52202/069179-0449

# 4 STRUCTURAL ANALYSIS

## 4.1 OVERVIEW OF THE ANALYTICAL MODEL

The analytical model is the same as the test body, with SN, SJ, DN, and DJ. An example of an analytical model is portrayed in Fig. 12. The wall has 910 mm length and 2730 mm height. The model replaced the members with wires, with nodal springs placed at each joint. Rotational springs were incorporated at the column-head joints and at the column-leg joints. The braces were placed with axial springs according to the direction of the applied force. Braces were designed so that, because of horizontal loads, the braces would push the beams upward when compression forces were applied. The top edge of the brace was kept close to the right edge of the beam. To reproduce effects of the L-shaped brace fastening metal, shear springs were placed to connect the top end of the brace to the top end of the column. For the SJ and DJ analytical models, rotational springs were set at the beam connections. To simplify the analytical model, the inter-columns were not modeled. Structural analysis was performed using software (Wallstat pro ver. 5.0.0β10) [9].

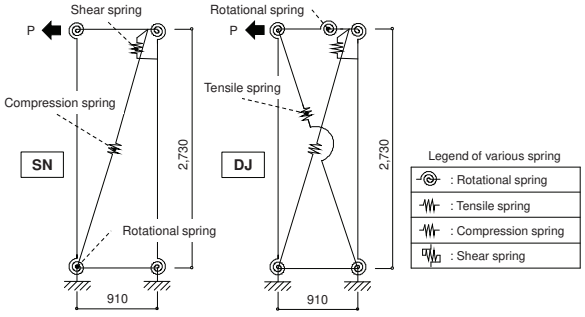


***Figure 12:*** *Analytical model example (unit: mm)*

## 4.2 JOINT STIFFNESS AND INFLECTION POINTS

In-plane rotation tests were applied to calculate the rotational stiffness of the column head-column leg joint. The test body configuration of the column head is shown at the left panel of Fig. 13. The test body configuration of the column leg is shown in the right panel. Fig. 13 shows that the applied forces were alternating positive and negative. The rotation angle of the joint was calculated from the values of two displacement gauges, as presented in Fig. 14. The number of test bodies was six for both the column head and the column leg joints. The relation between the moments and joint rotation angles of the six bodies and the skeletal curves created based on the test results is presented in Fig. 15. The initial and secondary stiffnesses of the six bodies are presented in Table 6.

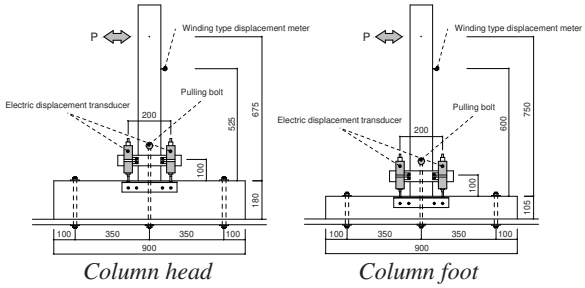


***Figure 13:*** *In-plane rotation test configuration (unit: mm)*

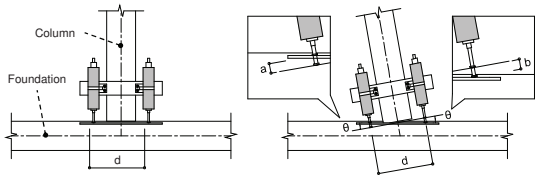


$\theta = ( a - b ) / d$

$\theta$: Relative displacement angle of two members (rad)
$a,b$: Displacement by displacement meter (mm)
$d$: Distance between gauge points (mm)

***Figure 14:*** *Calculation method of rotation angle of column-head and column-foot joint*

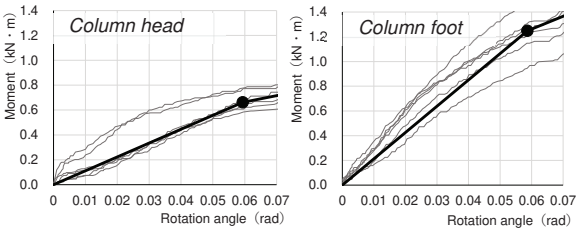


***Figure 15:*** *Relation between moment and rotation angle of column-head and column-foot joint*

***Table 6:*** *List of rotational rigidity in column-head and column-foot joint*

*Column head*

| Test piece number | Primary stiffness (kN・m/rad) | Secondary stiffness (kN・m/rad) |
|---|---|---|
| 1 | 11.3 | 5.7 |
| 2 | 12.0 | 5.0 |
| 3 | 11.2 | 4.8 |
| 4 | 9.9 | 5.1 |
| 5 | 10.9 | 4.5 |
| 6 | 11.5 | 5.2 |
| **Average** | **11.1** | **5.0** |
| **Standard deviation** | **0.6** | **0.4** |

*Column foot*

| Test piece number | Primary stiffness (kN・m/rad) | Secondary stiffness (kN・m/rad) |
|---|---|---|
| 1 | 26.4 | 12.4 |
| 2 | 22.0 | 11.0 |
| 3 | 20.1 | 9.2 |
| 4 | 21.4 | 8.1 |
| 5 | 21.2 | 12.1 |
| 6 | 16.5 | 9.5 |
| **Average** | **21.3** | **10.4** |
| **Standard deviation** | **2.9** | **1.6** |

Axial force tests were conducted to elucidate the joint characteristics. The test bodies were constructed as presented in Fig. 16 with six test bodies. The axial force test results are shown in Table 7: the average values of tensile and compressive stiffness were, respectively, 23.0 kN/mm and 45.1 kN/mm. The rotational stiffness of the joint was calculated using the tensile and compressive stiffnesses obtained from axial force test results. The rotational stiffness (mountainous deformation) calculation method is depicted in Fig. 18. In the case of bending deformation of a joint, tension is borne by part A and compression by part B. The stiffness per unit area was calculated by dividing the tensile and compressive stiffnesses shown in Table 7 by the respective bearing area. The calculation results show that the stiffness per unit area was 16.7 N/mm$^3$ on the tensile side and 2.9 N/mm$^3$ on the compressive side. The neutral axis was found to be 82.5 mm from the bottom edge by solving the equation of equilibrium between the tension and compression sides. Therefore, the rotational stiffness is calculated as the sum of tensile and compressive forces, 127 kN.m/rad, assuming that the stress level increases uniformly from the neutral axis to the outermost circumference.

https://doi.org/10.52202/069179-0449

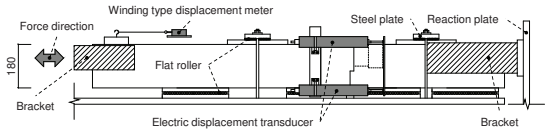


***Figure 16:*** *Axial force test configuration (unit: mm)*

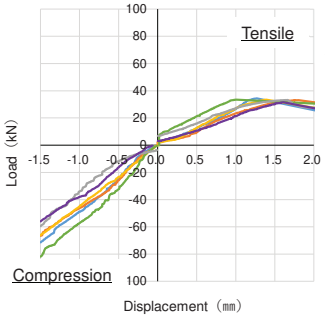


***Table 7:*** *List of test results (Tensile and compressive stiffness)*

| No. | Tensile stiffness (kN/mm) | Compressive stiffness (kN/mm) |
|---|---|---|
| 1 | 26.9 | 49.4 |
| 2 | 20.1 | 44.4 |
| 3 | 26.1 | 44.1 |
| 4 | 27.8 | 53.8 |
| 5 | 18.0 | 39.0 |
| 6 | 19.3 | 40.1 |
| **Average** | **23.0** | **45.1** |
| **Standard deviation** | **4.0** | **5.1** |

***Figure 17:*** *Relation between load and displacement for axial force test*

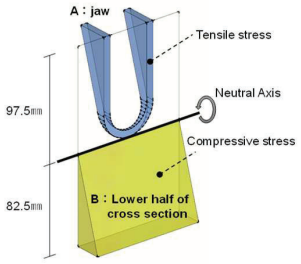


Tensile stiffness: 23.0 kN/mm
Pressure receiving area under tension: 1,381 mm$^2$
Tensile stiffness per unit area: 23.0 / 1,381 = 16.7 N/mm$^3$

Compressive stiffness: 45.1 kN/mm
Pressure receiving area under compression: 15,628 mm$^2$
Compressive stiffness per unit area: 45.1 / 15,628 = 2.9 N/ mm$^3$

***Figure 18:*** *Method of calculation rotational stiffness of beam joints*

The compressive stiffness of the single brace was ascertained from the load–displacement relation: the results of the analysis of the frame model consisting of rotational spring at the column-head-column-foot joint were subtracted from the in-plane shear test results obtained for the brace wall (average of three bodies) in Chapter 3 (Fig. 19).

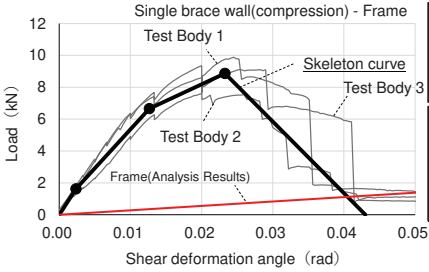


| | Stiffness (kN/rad) |
|---|---|
| 1st | 687 |
| 2nd | 489 |
| 3rd | 208 |
| 4th | -450 |

| | Inflection point displacement (rad) |
|---|---|
| 1st | 0.002 |
| 2nd | 0.013 |
| 3rd | 0.023 |
| 4th | 0.043 |

***Figure 19:*** *Skeleton curve of compression brace in a single-braced wall*

The tensile stiffness of the brace portrayed in Fig. 20 was found by subtracting the analytical results obtained for the frame model consisting of rotational spring at the column head-column leg connections from the in-plane shear test results (average of three bodies) of the tensile brace wall shown in the same figure.

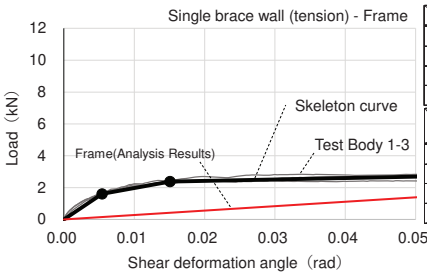


| | Stiffness (kN/rad) |
|---|---|
| 1st | 296 |
| 2nd | 80 |
| 3rd | 9 |
| 4th | -79 |

| | Inflection point displacement (rad) |
|---|---|
| 1st | 0.005 |
| 2nd | 0.015 |
| 3rd | 0.051 |
| 4th | 0.085 |

***Figure 20:*** *Skeleton curve of tensile brace*

We calculated the shear stiffness of the L-shaped brace hardware applied to the analytical model from the axial force of the brace and the displacement of the brace end found from results of in-plane shear tests of the brace wall (average of three bodies) (Fig. 21).

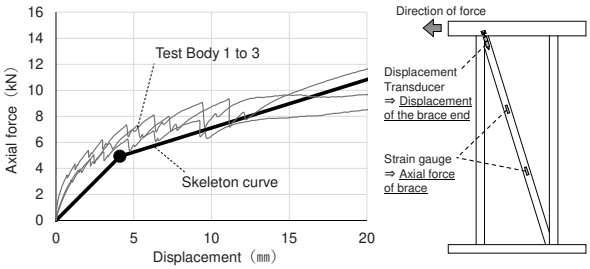


***Figure 21:*** *Skeleton curve of L-shaped brace hardware at the top edge of the brace*

The compressive stiffness of the double braces was calculated from the results of the in-plane shear tests described in Chapter 3 and from results obtained for the single braces. A compression brace in a double-braced wall has higher strength performance than a compression brace in a single-braced wall because the tensile brace in a double-braced wall delays buckling of the compression brace. However, the tensile brace performance was assumed to be equivalent to that of the single braces. The skeletal curves of the compression brace of the double-braced wall are presented in Fig. 22. From the in-plane shear test results obtained for the double-braced wall, the relation between the load and shear deformation angle of the frame and tensile bracing was subtracted to obtain the skeleton curve of the compression bracing of the double-braced wall.

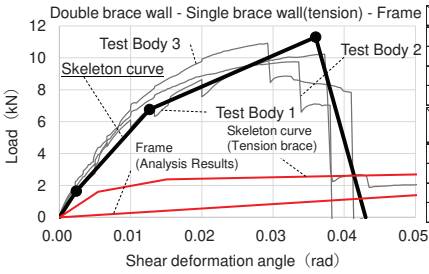


| | Stiffness (kN/rad) |
|---|---|
| 1st | 687 |
| 2nd | 489 |
| 3rd | 208 |
| 4th | -1645 |

| | Inflection point displacement (rad) |
|---|---|
| 1st | 0.002 |
| 2nd | 0.013 |
| 3rd | 0.036 |
| 4th | 0.043 |

***Figure 22:*** *Skeleton curve of compression brace in a double braced wall*


https://doi.org/10.52202/069179-0449

### 4.3 COMPARISON OF ANALYTICAL AND TEST RESULTS

Fig. 23 presents test results for each parameter and the analytically obtained results of the model with the previously described characteristic values. The test results and analysis results show general agreement. The developed analysis model is inferred as reasonable.

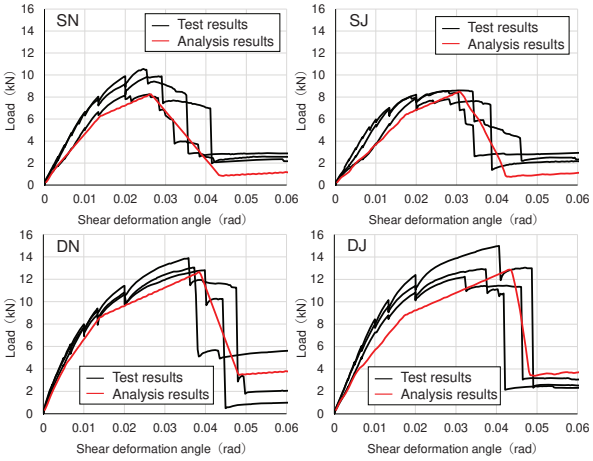


***Figure 23:*** *Relation between load and shear deformation angle in test and analysis*

Fig. 24 presents analytical results obtained for single-braced and double-braced walls. Fig. 25 shows the strength properties obtained from Fig. 24 and the test results. From Fig. 25, the maximum load was almost identical in the test and analytical results. Regarding the initial stiffness, the analytical results showed smaller values than the test results, but the tendency of the initial stiffness to decrease with the joint was similar. The test and analysis results demonstrated that the initial beam stiffness was reduced when the beam joint was placed at the push up of the brace, although it did not affect the maximum load.

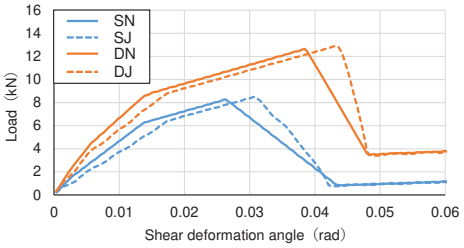


***Figure 24:*** *Relation between load and shear deformation angle in analytical results*

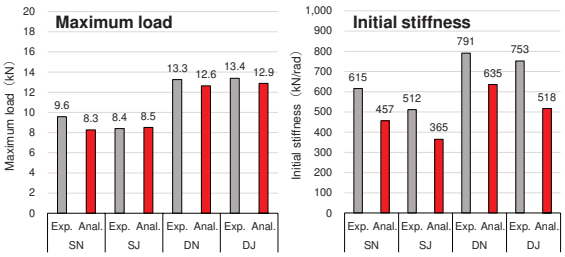


***Figure 25:*** *Maximum load and initial stiffness of analytical and test results*

## 5 CONCLUSIONS

A survey was administered to frame designers. The responses indicated that more than 70% of frame designers have concerns about a beam joint at the push-up portion of the brace. In-plane shear tests of single-braced and double-braced walls were conducted. The applied force test results indicated reduction of the initial stiffness of the single-braced, 910-mm-long wall by approximately 20% when the beam joint was placed at the push-up portion of the brace. Structural analyses were conducted by creating an analytical model of the braced wall. Those analyses revealed a similar trend to that indicated by the experimentally obtained results, thereby confirming the beam joint influence analytically.

## REFERENCES


[1] Independent administrative agency Housing Finance Support Organization, Wooden house construction specifications book, Inoue Shoin, 2016.

[2] City of Yokohama, Architecture Bureau guidance department architecture planning section, Seismic retrofit and construction of existing wooden houses manual (2009 Edition – Second Printing), reference 2023.1.9

[3] T. Sahata, N. Kawai, H. Tsukazaki, H. Maekawa, and S. Matsudome, Study on frame design in wooden house with machined members, Summaries of technical papers of Annual Meeting, Architectural Institute of Japan, pp. 211-212, 2019

[4] A. Nishino, N. Satomura, T. Taguchi, and Y. Ohashi, Study on aseismic repair method of cross wooden brace in the same plane. (Part 2 the difference in strength depending on the tree types of the wooden brace), Summaries of technical papers of Annual Meeting, Architectural Institute of Japan, pp. 535-536, 2019.

[5] Y. Nomura, K. Kanda, Y. Yamazaki, H. Sakata, and H. Isoda, Experimental study on mechanical behavior of wooden brace wall with different types of brace joint Part 1. Outline of experiments and failure mode, Summaries of technical papers of Annual Meeting, Architectural Institute of Japan, pp. 189-190, 2017.

[6] S. Sato, E. Fujino, and Y. Ohashi, A study on tensile strength of conventional wooden joints Part 1. koshikakekama-tsugi, Summaries of technical papers of Annual Meeting, Architectural Institute of Japan, pp. 97-98, 2002.

[7] Y. Kitada, and Y. Owada, A study on strength of conventional wooden joints – A tensile test of koshikakekamatsugite and okkakedaisentsugi-, Summaries of technical papers of Annual Meeting, Architectural Institute of Japan, pp.133-134, 2007.

[8] Public interest incorporated foundation Japan Housing and Wood Technology Center, Allowable stress design of wooden framed houses, 2017.

[9] T. Nakagawa, and M. Ohta,et al. "Collapsing process simulations of timber structures under dynamic loading III: Numerical simulations of the real size wooden houses", Journal of Wood Science, Vol. 56, No. 4, pp. 284-292, 2010.


https://doi.org/10.52202/069179-0449